Spin trapping and flipping in FeCO through relativistic electron dynamics

Journal:	*Physical Chemistry Chemical Physics*
Manuscript ID	CP-ART-10-2018-006583.R1
Article Type:	Paper
Date Submitted by the Author:	17-Dec-2018
Complete List of Authors:	Ulusoy, Inga; Michigan State University, Department of Chemistry Wilson, Angela; Michigan State University, Department of Chemistry

PCCP

ROYAL SOCIETY OF CHEMISTRY

ARTICLE TYPE

Cite this: DOI: 10.1039/xxxxxxxxxx

Spin trapping and flipping in FeCO through relativistic electron dynamics†

Inga S. Ulusoy*[a] and Angela K. Wilson‡[a]

Received Date
Accepted Date

DOI: 10.1039/xxxxxxxxxx

www.rsc.org/journalname

Transition metal compounds are very versatile, and their characteristics can differ profoundly depending on their electronic structure. Compounds in which a spin transition from a low-spin to a high-spin state can be achieved through means of an optical excitation are particularly intriguing, as a controlled spin-flip opens promising avenues in areas such as sensing, information technology, molecular switches and energy technology. The fundamental mechanisms in spin crossover and spin transitions remain unanswered, due to the complexity of electronic structure and interplay of relativistic effects. Presented here is a new approach that allows the first direct study of spin flip dynamics through a mapping of spin-mixed to spin-pure states. The method is applied to FeCO and addresses the spin-flip dynamics during a spin transition. Wave packets that combine different spin states are generated through optical excitation and relevant mechanisms in optically triggered spin transitions are discussed.

1 Introduction

Transition metal compounds are very versatile, and their characteristics can differ profoundly depending on their electronic configuration. Through the accessibility of different spin states, the macroscopic properties such as magnetic, optical, structural and crystallographic characteristics can vary drastically, which makes transition metal compounds promising candidates in areas such as sensing, information technology, molecular switches and energy technology.[1–3] Spin crossover and other spin-state conversion compounds, in which a transition from a low-spin (LS) to a high-spin (HS) state through means such as a thermal or optical excitation can be achieved, are key to the above applications. The question as to the fundamental mechanism in such spin transitions still remains unanswered due to the complexity and challenging nature of the electronic structure and interplay of relativistic effects[4,5]. Of particular interest are processes that are triggered by light, for example, in light-induced spin flip during LIESST (light-induced excited state spin trapping), reverse-LIESST, and in photocatalytic processes, as a controlled achievement of the targeted process (or a suppression of an undesired process) enables the design of new functional materials. Computational studies of transition metal compounds that exhibit spin-state conversion usually make use of time-independent approaches, in particular, using density functional theory (DFT),[6] CASSPT2 and CASSCF, and combined approaches.[5,7–14] To describe the electronic structure of transition metal compounds properly, a balanced description of static and dynamic correlation, as well as exchange effects has to be achieved. While DFT approaches can reproduce the properties of transition metal compounds accurately, their performance is not entirely predictable. Even more so, when also the electronic excited stateslb are to be studied, which can be of charge-transfer type, it is not apparent whether the selected functional and basis set are reproducing all electronic states with the targeted accuracy. If however a wave-function based approach is taken, then the approach can be systematically improved towards the exact representation. Presented here is the first explicitly time-dependent method that allows the study of spin flip dynamics through a mapping of spin-mixed to spin-pure states, thus providing instantanous insights into the electronic structure, charge migration and light-matter interaction. Electron motion and light-matter interactions can be studied through explicitly time-dependent methods, such as real-time time-dependent density functional theory (RT-TDDFT);[15] the algebraic diagrammatic construction scheme (ADC);[16,17] time-dependent configuration interaction (TDCI);[18] and the multiconfiguration time-dependent Hartree-Fock method (MCTDHF).[19–21] Spin-coupled electron dynamics has not been studied widely since this requires a relativistic treatment: Any process that leads to a spin flip and therefore a change in spin

[a] Department of Chemistry, Michigan State University, 578 S Shaw Lane, East Lansing MI 48824-1322, USA. Tel: +1 517 3531111.
* E-mail: ulusoyin@chemistry.msu.edu
‡ E-mail: wilson@chemistry.msu.edu

† Electronic Supplementary Information (ESI) available: [details of any supplementary information available should be included here]. See DOI: 10.1039/cXCP00000x/

multiplicity is only possible through spin-orbit coupling (SOC). As SOC is a relativistic effect, the spin-coupled dynamics can only be described by a relativistic Hamiltonian.

Only one of the above explicitly time-dependent methods has been combined with a relativistic description, that is, using the electron density to describe the electron dynamics as in exact two-component TDDFT (X2-TDDFT),[22–25] and using a density-matrix formalism.[26,27] Another framework that can be combined with linear-response TDDFT or equation-of-motion coupled cluster (EOM-CC) theory, for example, is the spin flip (SF) approach by A. Krylov.[28–32] Here, determinants corresponding to different spin multiplicites are either generated directly from a reference determinant, or more general spin-flip operators can be used.

The approach taken in the work presented here originates in the perspective of transition metal chemistry, in particular, focusing on electronic excited states that play a role in transition metal compounds during spin trapping processes such as LIESST. For this, a balanced description of static and dynamic correlation, as well as exchange effects has to be achieved, not only of the ground, but also excited states which often are of charge-transfer type. Furthermore, the electric field coupling needs to be described in a time-dependent framework, beyond equation of motion or linear response theories. The developed methodology is applied to address the spin-coupled electron dynamics in FeCO. The FeCO compound exhibits several low-lying states of same angular momentum but different spin multiplicity, and wave packets that combine different spin multiplicities can be generated through optical excitation. These superposition states combine two different spin states and result in time-dependent spin multiplicities, electron and spin densities, and spin orbital (SO) occupations. By examining the content of spin-pure contributions to the spin-mixed states, pathways and mechanisms that may be relevant in optically triggered spin processes are discussed.

2 Time-dependent spin-orbit configuration interaction

Here, we present a first combination of the TDCI methodology with a relativistic Hamiltonian. Recently, a density-matrix based TDCI approach has been presented and applied to the spin dynamics in $[Fe(H_2O)_6]^{2+}$, for the computation of X-ray absorption spectra and Auger decay.[33] Our approach retains the wave function representation instead of the density and allows for a mapping of properties on the molecular orbital (MO) or determinant picture at all time steps. As such, an interpretation of the results remains chemically intuitive and allows a deeper understanding of the underlying mechanism and influencing factors in the spin-flip dynamics.

The time-dependent spin-orbit CI (TD-SOCI) approach is built from the TDCI approach, but the wave function is expanded using a SOC Hamiltonian.[34,35] We make use of the implementation available in GAMESS-US,[34,35] the Breit-Pauli SOC Hamiltonian

$$\hat{H}^{\mathrm{BP}}_{\mathrm{SOC}} = \frac{1}{2m^2c^2}\left[\sum_i\sum_A \frac{Z_A e^2}{r_{iA}}\hat{l}_{iA}\cdot\hat{s}_i - \sum_i\sum_j \frac{e^2}{r_{ij}^3}\hat{l}_{ij}\cdot(\hat{s}_i + 2\hat{s}_j)\right] \quad (1)$$

with $\hat{l}$ the space and $\hat{s}$ the spin angular momentum operator. In TDCI, the wave function is expanded in energy eigenstates with time-dependent coefficients,

$$|\Phi_{\mathrm{TDCI}}(t)\rangle = \sum_i^{\mathrm{nstates}} \mathrm{C}_i(t)|\Psi_i\rangle \quad (2)$$

and the Hamiltonian is a sum of the CI molecular Hamiltonian and a term for the electric field coupling in semi-classical and dipole approximation and length gauge.[36] For an extension to TD-SOCI, the propagation of coefficients is carried out in spin-mixed SOCI eigenstates, that is, a representation that diagonalizes $\hat{H}_{\mathrm{SOCI}} = \hat{H}_{\mathrm{CI}} + \hat{H}_{\mathrm{SOC}}$. Here, the coefficients $C^{\mathrm{S}}(t)$ denote the weight of the *spin-mixed* eigenstates i and are propagated using a split operator:

$$C_i^{\mathrm{S}}(t+\Delta t) = \left(e^{-i\mathbf{H}_{\mathrm{SOCI}}(t+\Delta t)}\mathbf{U}^{\dagger}e^{-i\boldsymbol{\mu}_p E_p(t+\Delta t)}\mathbf{U}\right)^{\mathrm{S}}_i C_i(t) \quad (3)$$

The electric field coupling is represented in position eigenstates, so that the matrix in the exponent, $\boldsymbol{\mu}_p$, contains only diagonal terms for each the cartesian directions $p = \{x,y,z\}$. The matrix $\mathbf{U}$ is used to transform back and forth between SOCI and position eigenstates in which each of the respective matrices is diagonal.

The matrix that diagonalizes the SOC Hamiltonian in the CI basis, $\mathbf{U}_{\mathrm{S}}$, can be used to map the time-dependent coefficients $C^{\mathrm{S}}(t)$ onto the spin-pure energy eigenstates $C(t)$,

$$C_i(t) = \mathbf{U}_{\mathrm{S}} C_i^{\mathrm{S}}(t) \quad (4)$$

Further, the coefficients of the spin-pure eigenstates relate the many-electron wave function to its constituting determinants, SOs and MOs. Through successive basis transformations, populations of MOs, bond orders, electron localization function, and the electronic flux density[37,38] can be constructed. As the propagation is carried out in SOCI eigenstates, there is no population transfer between the states as long as no electric field term is present. Once a laser pulse is "switched on", a coupling of the different SOCI states is achieved through the transition dipole moments that enable optical transitions between the states. A propagation with an electric field term then leads to population shifts of the SOCI eigenstates, and different occupation patterns of the MOs.

3 Computational details

The SO-CIS and SO-CISD[35,39–41] calculations of FeCO are carried out using Dunning's cc-pVTZ basis set[42,43] for both metal atom and ligands, and with an active space of 18 electrons in 18 MOs (SO-CIS(18,18) and SO-CISD(18,18)). The scalar relativistic effects are treated with the infinite-order two-component method.[44] and spin-orbit coupling through the Breit-Pauli spin-orbit Hamiltonian[35] (HSO2) as implemented in GAMESS-US.[34] All calculations are carried out at the experimental equilibrium geometry (r(Fe-C)=1.7270 Å and r(C-O)=1.1586 Å), and the 20 lowest-lying states of each spin multiplicity are included, resulting in 180 spin-coupled states when the J_z degeneracy is lifted.

The semiclassical dipole approximation is used and only dipole coupling is considered, while the higher-order terms can in principle result in non-negligible contributions.[22] At this point, ion-

ization is not considered, but extensions of the TDCI methodology in this respect are already available.[45] We make use of the gauge-variance of the CI approach to assess the convergence of the wave function.[36] All calculations are carried out with the nuclei kept frozen at the specified positions, as the time scales that are targeted are expected to lie below the onset of nuclear motion for atoms heavier than hydrogen (typically faster than 50-80 fs),[46–48] though for traditional spin-crossover and spin-transition materials, the nuclear coordinates are fundamental and have to be included explicitly in a modeling of the complete spin transition from LS to HS. For the compound and time scales in this study, the nuclear motion is expected to play a lesser role, as the bond length change associated with the HS is smaller with 0.1 Å and there is only one ligand, thus the net volume change is significantly smaller. However, some of the energetic ordering of the excited Π and Δ states changes, possibly enhancing the intermixing of states with the change of nuclear coordinate,[49] and possibly leading to an enhancement of the features discussed below.

4 Spin-orbit coupled electron dynamics in FeCO

Using this newly developed methodology, the spin-mixed electron dynamics in FeCO can be studied. FeCO is known to be notoriously difficult to describe theoretically with a triplet ground state and a very close-lying quintet state. Theoretical methods have largely failed at reproducing the correct ordering of the electronic states.[49] The experimental rovibrational energy difference between the two lowest-lying states of different multiplicity is only 1135 cm^{-1}, with the LS state being the ground state. Typically, the zero-point vibrational energy for the HS state is lower than for the LS state, due to the shorter and more rigid metal-ligand bonds in the LS state. Taking this into account, the purely electronic energy difference between LS and HS is even smaller, and has been predicted[49] to lie between ≈ 450-500 cm^{-1}. The incorrect prediction of this energy difference through theoretical methods is ascribed to an insufficient dynamical correlation treatment. Our SOCI results are consistent with these findings: At the SO-CIS(18,18)/cc-pVTZ level, the ordering of electronic states is prediced incorrectly, with the $^5\Sigma$ HS state being the lowest electronic state (7900 cm^{-1} below the $^3\Sigma$ state). Including dynamic correlation through a CISD expansion, the correct state ordering is retained with a vertical electronic energy difference of LS and HS as 320 cm^{-1}. In the following, only the SO-CISD(18,18) wave function is used as initial state for the TD-SOCI calculation. Relative electronic energies and dipole moments for the lowest-lying SOCI multiplets are given in Fig. 1, and the agreement with literature values is very good,[49] with only a few tenths of wavenumbers difference in the energies, and typical differences of about 0.1-0.2 D in the dipole moments.

Already for comparatively low energy differences as in the region between 12,000-16,000 cm^{-1}, the density of electronic states is high. With increasing total orbital angular momentum L (where Σ corresponds to $L = 0$, Π to $L = 1$, Δ to $L = 2$, Φ to $L = 3$ as denoted in Fig. 1), the energy differences between the spin-orbit multiplets (of which there are three for the triplet,

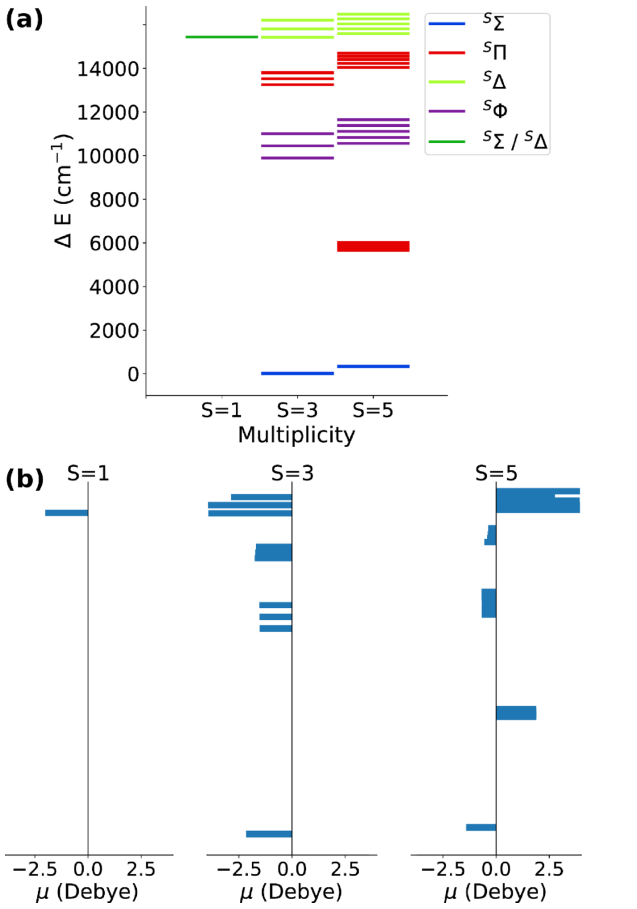

Fig. 1 (a) Relative energies of the SOCI multiplets with respect to the electronic ground state. **(b)** Dipole moments of the SOCI states, where a negative dipole moment corresponds to positive partial charges on iron and partial negative charges on oxygen.

and five for the quintet states) becomes more pronounced. With this, the Δ-states for triplet and quintet multiplicity lie close in energy. The only bound singlet state lies much higher in energy at 15442 cm^{-1}. Comparing the dipole moments of the low-lying electronic states, the dipole moment in the $X^3\Sigma$ ground state is large with a negative sign, corresponding to a direction of the vector from the metal center to the ligand. The metal atom is slightly positively charged, as is the carbon atom, while there is a partial negative charge on the oxygen atom. The bonding in FeCO has been discussed previously,[49] and the most relevant molecular orbitals (MOs) are shown in the Supporting Information. In the triplet ground state, σ-donation from the ligand to the metal atom through the 11σ MO and π-backdonation from the metal atom to the ligand through the 4π MO leads to a net charge transfer to the ligand. The σ-donation is weakend in the quintet state, as here one of the electrons of the σ-donating MO is promoted to the antibonding 12σ MO. This results in a dipole moment of the lowest-lying HS state that is smaller in magnitude than the one of the LS ground state. Notable also is that the dipole moments of the $^5\Pi$ and $^5\Delta$ states are large with a positive sign, corresponding to a reversed charge distribution in the compound.

In Fig. 2, the optically accessible electronic excited states start-

ing from the triplet ground state T_0 and the lowest-lying quintet state Q_0 are illustrated (possible transitions from the lowest-lying singlet state S_0 are given in the Supporting Information, as this state lies comparatively high in energy). The energy difference is represented on the y-axis relative to the triplet ground state, and the magnitude of the transition dipole moment, which dictates the coupling between initial and final state, is represented through the size of the circles. The accessible excited states are classified according to their spin multiplicity by different colors. The transition dipole moments between the low-lying bound states are rather low, even for the $^3\Pi \leftarrow X^3\Sigma$ transition. However, transitions to high-lying states above the ionization threshold exibit larger oscillator strengths (f $\approx$ 0.2 with an energy difference of 35,000 cm^{-1} to 50,000 cm^{-1}). Optical (de-)excitations that involve a spin flip are predominantly possible from S_0, while from T_0 still a few spin flip excitations can be observed. However, from the lowest-lying quintet state, there are almost no spin-flip transitions possible; almost all optical transitions from Q_0 are to higher-lying quintet state. This characteristic is expected to play a crucial role in spin trapping — as the spin multiplicity changes to higher multiplicities through optical excitations and spin-flip, the reverse process cannot be induced as easily.

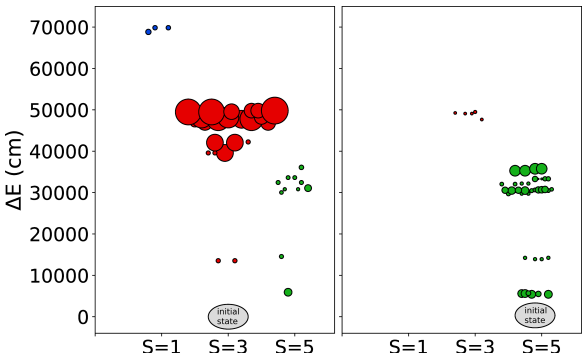

Fig. 2 Electronic excitations out of the triplet ground state T_0 (left) and the lowest-lying quintet state Q_0 (right), that can be induced optically. For each multiplicity, the initial state is marked with grey, while the accessible excited states are classified according to their spin multiplicity (blue – singlet, red – triplet, green – quintet), and the magnitude of the transition dipole moment is reflected through the size of the circles. The y-axis corresponds to the relative energy of the electronic states with respect to the triplet ground state.

In the following, a different perspective on the spin-coupled dynamics is adopted, as the propagation is carried out in spin-mixed $\hat{H}_{\mathrm{SOCI}}$ eigenstates. In the spin-coupled framework, each electronic state is no longer a spin-pure state, but contains contributions of other spin states. In this way, an accumulation of contribution to the spin-other states can be seen as a partial "spin flip" in the spin-pure CI energy eigenstates. While the propagation is carried out in spin-mixed states, the state populations can be transformed back into spin-pure states to determine the admixture of spin-other states in that representation.

In Table 1, the admixture of singlet, triplet and quintet states to the spin-mixed states are given as $\%C(S=3) = \sum_i |C_i(S=3)|^2 \cdot 100$, and correspondingly for the other multiplicities. Transforming the population of the spin-mixed eigenstates back into spin-pure eigenstates, it becomes apparent that, for example, the $^5\Delta_1$ state contains contributions of triplet states in the spin-pure basis, and quite significantly so. In fact, the $^5\Delta_1$ state contains almost 28% contributions of triplet states in the spin-pure CI basis.

Table 1 Admixture of singlet, triplet, and quintet multiplicity in the spin-pure representation to the low-lying spin-mixed electronic states of FeCO.

State	$\%C(S=1)$	$\%C(S=3)$	$\%C(S=5)$
$^3\Sigma_0$	0.38	99.54	0.08
$^3\Sigma_1$	0.01	99.72	0.27
$^5\Sigma_{0,1,2}$	0.00	0.00	100.00
$^5\Pi_{3,2,1}$	0.00	0.02	99.98
$^5\Pi_1$	0.01	0.64	99.36
$^5\Pi_0$	0.00	0.48	99.52
$^3\Phi_{4,3}$	0.74	99.16	0.10
$^5\Phi_{5,4}$	0.00	0.00	100.00
⋮	⋮	⋮	⋮
$^3\Pi_2$	0.98	78.94	20.08
$^3\Pi_1$	0.17	79.41	20.43
⋮	⋮	⋮	⋮
$^1\Sigma_{3,7}/^1\Delta_{3,7}$	99.17	0.80	0.04
⋮	⋮	⋮	⋮
$^3\Delta_1$	0.00	94.93	5.07
$^5\Delta_1$	0.00	29.97	70.03
$^5\Delta_0$	0.00	7.14	92.86
$^3\Delta_1$	1.15	7.39	91.46

In Fig. 3, a propagation of the $^5\Delta_1$ state without an electric field term is shown. The state population $|C_i(t)|^2$ thus remains constant as 1.0, while the imaginary and real part or the CI coefficient oscillate with a frequency that corresponds to the relative energy of the state (as $C_i^S(t+\Delta t) = e^{-iE_i(t+\Delta t)}C_i^S(t)$). Transforming the population of the spin-mixed eigenstate back into spin-pure eigenstates, the *approx*28% contributions of triplet states in the spin-pure CI basis become apparent. Especially the higher-lying triplet and quintet Δ-states exhibit strong SOC, splitting of the SOCI multiplets, and significant admixtures of spin-other states in the spin-pure basis. The low-lying triplet and quintet states however retain spin purity almost completely (especially the quintet states). This absence of admixture of spin-other states could be another factor in the "spin trapping" in some transition metal compounds.

However, can a spin flip be induced directly through an optical excitation? A comparison of transition dipole moments from the triplet ground state to quintet excited states does indeed provide a promising target, a low-lying $^5\Pi$ state. The transition dipole moment along the molecular axis is $\mu = 0.208$ D for a $^5\Pi \leftarrow X^3\Sigma$ transition. A propagation is carried out with an electric field term, where the molecule is irradiated with a resonant laser pulse (the pulse frequency corresponds to the energy difference between initial and target state, $\omega = 5917\,cm^{-1}$). The maximum field strength is $7.9\,e^{12}$ W/cm^2 for a $\cos^2$ pulse envelope with a laser

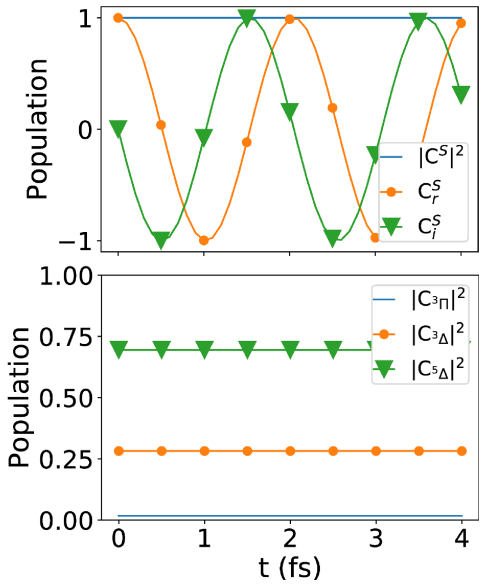

Fig. 3 State populations in spin-mixed C^S and spin-pure C energy eigenstates for the $^5\Delta_1$ state, without an electric field term in the Hamiltonian. Through the transformation from the spin-mixed into the spin-pure basis, it becomes apparent that this quintet state contains large admixtures of triplet spin multiplicity.

pulse about eight cycles in length (t_P = 45.0 fs). The populations of spin-mixed and spin-pure states are shown in Fig. 4.

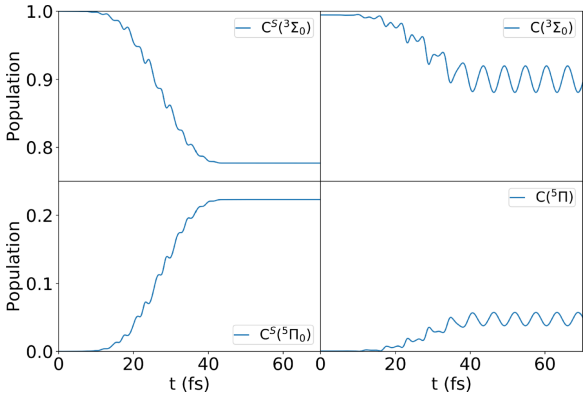

Fig. 4 State populations during and after irradiation with a resonant laser pulse of 45 fs length, where a transition between the $X^3\Sigma$ ground state and a low-lying $^5\Pi$ state is induced, in the representation of spin-mixed states $C^S(t)$ (left) and spin-pure states $C(t)$ (right). In this case, a population transfer of 24% in the spin-mixed basis corresponds to a population transfer of ≈4.1-6.2% in the spin-pure representation.

At the end of the laser pulse, about 24% population of the ground state has been transferred to the targeted excited state, thus leading to a superposition state that contains 76% $X^3\Sigma$ and 24% $^5\Pi$ contributions. Converting these populations into the spin-pure basis shows that this corresponds to a population of 87.5-91.6% of the spin-pure $^3\Sigma$ state and 4.1-6.2% of the spin-pure $^5\Pi$ state. As the final state after the laser pulse excitation is a superposition state, a wave packet has been generated that combines eigenstates originating in two different spin multiplicities. As a wave packet leads to a non-stationary electron distribution in the molecule, an overall charge migration and time-dependent properties are obtained.[50] This is reflected in the oscillations of the spin-pure coefficients that vary on a time scale of about 6 fs.

Throughout the propagation, not only state populations are monitored, but also SO occupancies through the one-particle reduced density matrix. This allows an identification of electronic pathways, and time-dependent expectation values such as dipole moments and electron density. In the $^5\Pi \leftarrow X^3\Sigma$ transition that is targeted above, one electron is promoted from one of the 4π MOs to the 12σ MO and undergoes a spin flip (see Supporting Information). The occupancy of the relevant SOs during the propagation is shown in Fig. 5(a). The electron occupation of the $4\pi^\alpha$ and $12\sigma^\beta$ SOs remains constant while there is a net charge transfer between the $4\pi^\beta$ and $12\sigma^\alpha$ SOs. After the wave packet has been generated, oscillations on the same time scale as for the state coefficients are observed, resulting from the non-stationary nature of a wave packet.

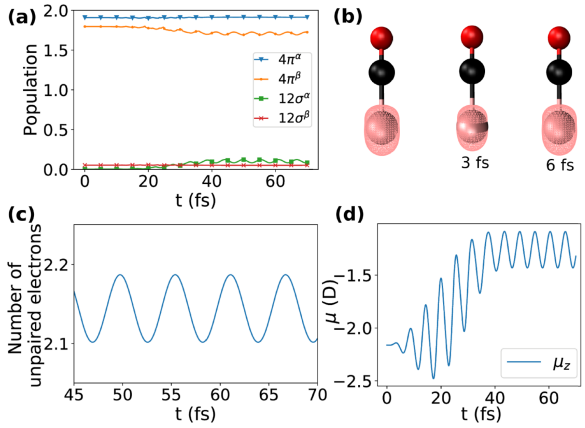

Fig. 5 (a) Occupancies of relevant α and β SOs during laser pulse excitation with induced spin flip. The occupancy of the $4\pi^\alpha$ and $12\sigma^\beta$ SOs remains constant while there is an occupancy transfer between the $4\pi^\beta$ and $12\sigma^\alpha$ SOs. **(b)** The spin density difference in FeCO oscillates after generation of the wave packet. The spin density difference is localized on the Fe atom. **(c)** The number of unpaired electrons after the wave packet has been generated by optical excitation. Through the time-dependent wave packet, a time-dependent multiplicity is generated as the number of unpaired electrons oscillates. The resulting overall multiplicity varies between 3.1 and 3.2 with an oscillation period of 6 fs. **(d)** The time-dependent dipole moment changes throughout the excitation and oscillates after the wave packet has been generated, signifying a charge migration in the compound.

The resulting time-dependent difference in electronic spin density is shown in Fig. 5(b). The spin density difference is localized on the Fe atom and oscillates on the same time scale as the coefficients and populations. Taking the difference of the sum of all α and β occupancies reveals that the number of unpaired electrons oscillates between 2.1 and 2.2 (Fig. 5(c)), resulting in a spin multiplicity of the wave packet that is predominantly triplet and varies between 3.1 and 3.2 on a femtosecond time scale.

In Fig. 5(d), the time-dependent dipole moment of FeCO during the propagation is shown. Initially, the dipole moment is decreased in magnitude, due to the population of the quintet state

in which the charge donation and back-donation between CO and Fe is reduced. After the wave packet has been generated and the laser pulse has been switched off, charge migration occurs as a consequence of the time-dependent superposition state, resulting in an oscillating dipole moment.

5 Conclusions

A routine was developed to include spin-orbit coupling in a time-dependent framework of electronic structure theory. Through the wave function representation of the system, electronic states in spin-mixed and spin-pure basis are accessible at all time steps, and can be related back to the MO (SO) representation. Through a comparison of spin-mixed and spin-pure states, the spin admixtures can be analyzed. The higher-lying electronic states with larger angular momentum exhibit significant spin-orbit coupling and spin admixtures of spin-other states, of up to 28%. This implies that after optical excitation and relaxation to one of these states, a spin flip can easily be initiated as the transition dipole moments and the contributions of spin-other states are large. However, from the triplet ground state, and even more so the quintet ground state, a direct optical route from LS to HS (and vice versa) is not accessible for this compound. A partial conversion from triplet to quintet multiplicity could be achieved by targeting the $^5\Pi \leftarrow X^3\Sigma$ transition. After the laser pulse, a wave packet has been generated that is a superposition of initial triplet and quintet target state. Transforming the coefficients back into spin-pure eigenstates reveals that the quintet contributions is at most 6% in this case.

As a result of our study, several characteristics that will play a role in spin flipping and trapping in compounds with optical spin state transitions have been identified. For one, the higher-lying bound triplet and quintet states exhibit significant SOC and, induced through this coupling of spin and momentum, can contain quite large admixtures of spin-other states. Transitions between these states can be induced easily through optical means, and they present the "channels" that enable spin flipping. Further, the lowest-lying quintet state acts as a "sink", in that it exhibits weak dipole coupling of quintet ground and quintet (even more so, triplet and singlet) excited states. Once the spin flip to quintet multiplicity takes place, relaxation through internal conversion is likely, and once the lowest-lying quintet state is reached, it is much more difficult to induce a spin flip.

Acknowledgement

We gratefully acknowledge financial support from the U.S. Department of Energy, Office of Science, Basic Energy Sciences under Award Grant DE-SC0017889. This work used the Extreme Science and Engineering Discovery Environment (XSEDE),[51] which is supported by NSF Grant Number ACI-1548562. The XSEDE resource Comet at the University of California, San Diego, was used for all calculations through allocation TG-CHE170014.

6 Additional Information

Supplementary Information is available is available for this paper at xxx.

References

1 *Spin-Crossover Materials Properties and Applications*, ed. M. A. Halcrow, John Wiley & Sons Ltd, 2013.
2 P. Gütlich, A. Hauser and H. Spiering, *Angew. Chemie Int. Ed. English*, 1994, **33**, 2024–2054.
3 A. Marino, P. Chakraborty, M. Servol, M. Lorenc, E. Collet and A. Hauser, *Angew. Chemie - Int. Ed.*, 2014, **53**, 3863–3867.
4 W. Zhang, R. Alonso-Mori, U. Bergmann, C. Bressler, M. Chollet, A. Galler, W. Gawelda, R. G. Hadt, R. W. Hartsock, T. Kroll, K. S. Kjær, K. Kubiček, H. T. Lemke, H. W. Liang, D. A. Meyer, M. M. Nielsen, C. Purser, J. S. Robinson, E. I. Solomon, Z. Sun, D. Sokaras, T. B. van Driel, G. Vankó, T.-C. Weng, D. Zhu and K. J. Gaffney, *Nature*, 2014, **509**, 345–348.
5 M. Fumanal, E. Gindensperger and C. Daniel, *J. Phys. Chem. Lett*, 2018, **9**, 37.
6 H. Paulsen, V. Schünemann and J. A. Wolny, *Eur. J. Inorg. Chem.*, 2013, **2013**, 628–641.
7 B. O. Roos, K. Andersson, M. P. Fülscher, P.-â. Malmqvist, L. Serrano-Andrés, K. Pierloot and M. Merchán, *M. Merchán*, 2007, pp. 219–331.
8 D. Hagberg, E. Bednarz, N. M. Edelstein and L. Gagliardi, *J. AM. CHEM. SOC*, 2007, **129**, 58.
9 C. D. Graaf and C. Sousa, *J. Am. Chem. Soc.*, 2008, **130**, 13961–13968.
10 C. D. Graaf and C. Sousa, *Int. J. Quantum Chem.*, 2011, **111**, 3385–3393.
11 C. Sousa, C. de Graaf, A. Rudavskyi, R. Broer, J. Tatchen, M. Etinski and C. M. Marian, *Chem. Eur. J.*, 2013, **19**, 17541–17551.
12 C. Daniel, *Coord. Chem. Rev.*, 2015, **282-283**, 19–32.
13 V. Jovanovi, I. Lyskov, M. Kleinschmidt and C. M. Marian, *Mol. Phys.*, 2017, **115**, 109–137.
14 C. Sousa, A. Domingo and C. de Graaf, *Chem. - A Eur. J.*, 2018, **24**, 5146–5152.
15 M. R. Provorse and C. M. Isborn, *Int. J. Quant. Chem.*, 2016, **116**, 739–749.
16 A. I. Kuleff, J. Breidbach and L. S. Cederbaum, *J. Chem. Phys.*, 2005, **123**, 044111.
17 M. Pernpointner, L. Visscher and A. B. Trofimov, *J. Chem. Theory Comput.*, 2018, **14**, 1510–1522.
18 T. Klamroth, *Phys. Rev. B*, 2003, **68**, 245421.
19 T. Kato and H. Kono, *Chem. Phys. Lett.*, 2004, **392**, 533–540.
20 J. Caillat, J. Zanghellini, M. Kitzler, O. Koch, W. Kreuzer and A. Scrinzi, *Phys. Rev. A*, 2005, **71**, 012712.
21 M. Nest, T. Klamroth and P. Saalfrank, *J. Chem. Phys.*, 2005, **122**, 124102.
22 J. J. Goings, J. M. Kasper, F. Egidi, S. Sun and X. Li, *J. Chem. Phys.*, 2016, **145**, 104107.
23 J. M. Kasper, P. J. Lestrange, T. F. Stetina and X. Li, *J. Chem. Theory Comput.*, 2018, **14**, 1998–2006.
24 F. Egidi, S. Sun, J. J. Goings, G. Scalmani, M. J. Frisch and X. Li, *J. Chem. Theory Comput.*, 2017, **13**, 2591–2603.
25 W. Liu and Y. Xiao, *Chem. Soc. Rev.*, 2018, 4481–4509.

26 J. E. Peralta, O. Hod and G. E. Scuseria, *J. Chem. Theory Comput.*, 2015, **11**, 3661–3668.

27 M. Kadek, L. Konecny, B. Gao, M. Repisky and K. Ruud, *Phys. Chem. Chem. Phys.*, 2015, **17**, 22566–22570.

28 A. I. Krylov, *Chem. Phys. Lett.*, 2001, **338**, 375 – 384.

29 A. I. Krylov, *Chem. Phys. Lett.*, 2001, **350**, 522 – 530.

30 Y. Shao, M. Head-Gordon and A. I. Krylov, *J. Chem. Phys.*, 2003, **118**, 4807–4818.

31 S. V. Levchenko and A. I. Krylov, *J. Chem. Phys.*, 2004, **120**, 175–185.

32 E. Epifanovsky, K. Klein, S. Stopkowicz, J. Gauss and A. I. Krylov, *J. Chem. Phys.*, 2015, **143**, 064102.

33 H. Wang, S. I. Bokarev, S. G. Aziz and O. Kühn, *Mol. Phys.*, 2017, **115**, 1898–1907.

34 M. W. Schmidt, K. K. Baldridge, J. A. Boatz, S. T. Elbert, M. S. Gordon, J. H. Jensen, S. Koseki, N. Matsunaga, K. A. Nguyen, S. Su, T. L. Windus, M. Dupuis and J. A. Montgomery, *J. Comput. Chem.*, 1993, **14**, 1347–1363.

35 D. G. Fedorov, S. Koseki, M. W. Schmidt and M. S. Gordon, *Int. Rev. Phys. Chem.*, 2003, **22**, 551–592.

36 I. S. Ulusoy, Z. Stewart and A. K. Wilson, *J. Chem. Phys.*, 2018, **148**, 014107.

37 G. Hermann, C. Liu, J. Manz, B. Paulus, J. F. Pérez-Torres, V. Pohl and J. C. Tremblay, *J. Phys. Chem. A*, 2016, **120**, 5360–5369.

38 V. Pohl, G. Hermann and J. C. Tremblay, *J. Comp. Chem.*, 2017, **38**, 1515–1527.

39 B. Brooks and H. F. Schaefer, *J. Chem. Phys.*, 1979, **70**, 5092.

40 B. Brooks, W. Laidig, P. Saxe, N. Handy and H. F. Schaefer, *Phys. Scr.*, 1980, **21**, 312.

41 S. Koseki and M. S. Gordon, *J. Mol. Spectrosc.*, 1987, **123**, 392–404.

42 T. H. Dunning, Jr., *J. Chem. Phys.*, 1989, **90**, 1007–1023.

43 N. B. Balabanov and K. A. Peterson, *J. Chem. Phys*, 2005, **123**, 064107.

44 M. Barysz and A. J. Sadlej, *J. Chem. Phys.*, 2002, **116**, 2696–2704.

45 S. Klinkusch, P. Saalfrank and T. Klamroth, *J. Chem. Phys.*, 2009, **131**, 114304.

46 G. Auböck and M. Chergui, *Nature*, 2015, **7**, 629–633.

47 I. S. Ulusoy and M. Nest, *J. Phys. Chem. A*, 2012, **116**, 11107–11110.

48 A. J. Atkins and L. Gonzaíez, *J. Phys. Chem. Lett*, 2017, **8**, 13.

49 T. Hirano, R. Okuda, U. Nagashima and P. Jensen, *J. Chem. Phys.*, 2012, **137**, 244303.

50 L. S. Cederbaum and J. Zobeley, *Chem. Phys. Lett.*, 1999, **307**, 205–210.

51 J. Towns, T. Cockerill, M. Dahan, I. Foster, K. Gaither, A. Grimshaw, V. Hazlewood, S. Lathrop, D. Lifka, G. D. Peterson, R. Roskies, J. R. Scott and N. Wilkins-Diehr, *Comput. Sci. Eng.*, 2014, **16**, 62–74.

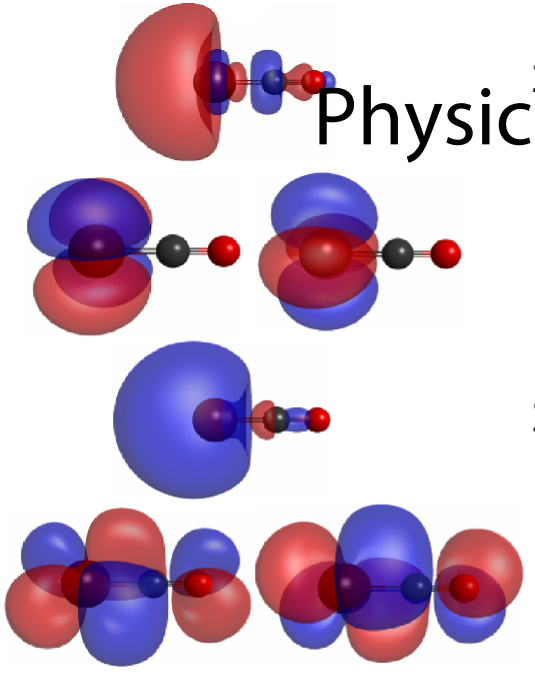

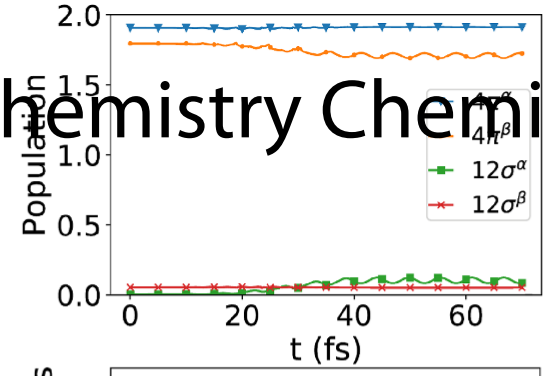

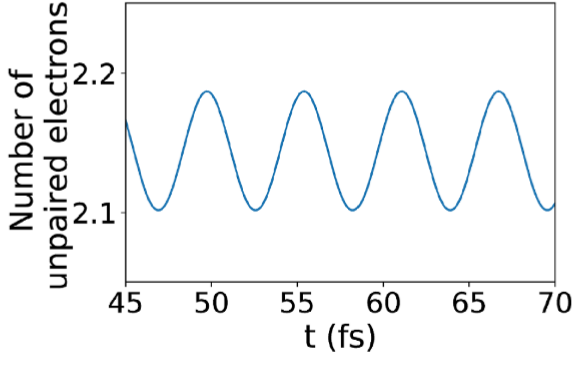

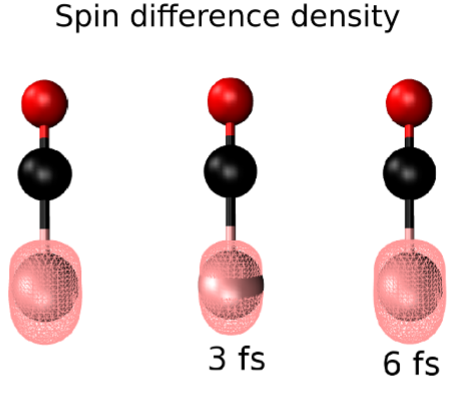

Electron dynamics of spin-state conversion compounds. Excited triplet and quintet states are significantly spin-mixed - transitions can be induced easily: ”channels” that enable spin flipping. The lowest-lying quintet state acts as a "sink”: exhibits weak coupling.